EFFECTS ON ELECTRICAL, THERMAL AND MECHANICAL PROPERTIES OF EPOXY RESINS REINFORCED WITH MICRO AND NANOFILLERS

A project report

Submitted
By

DASUPURAM MADHAVARAO
EE15M023

In partial fulfilment
of the requirements for the degree of

Master of Technology

DEPARTMENT OF ELECTRICAL ENGINEERING
INDIAN INSTITUTE OF TECHNOLOGY MADRAS
May 2017

CERTIFICATE

This is to certify that the report entitled, "**EFFECTS ON ELECTRICAL, THERMAL AND MECHANICAL PROPERTIES OF EPOXY RESINS BY ADDING MICRO AND NANOFILLERS",** submitted by **DASUPURAM MADHAVARAO, EE15M023**, to the Department of Electrical Engineering, Indian Institute of Technology Madras, for the award of the degree of **Master of Technology**, is a bona fide record of the research work carried out by him under my supervision. The contents of this project, in full or in parts, have not been submitted to any other Institute or University for the award of any degree or diploma.

Dr. R.Sarathi
Professor
Department of Electrical Engineering
Indian Institute of Technology Madras

Chennai

May , 2017

Abstract

High performance polymer nanocomposites are emerging as a new class of insulating materials for demanding application in all electrical equipment used in the outdoor/indoor power system network. Epoxy resins are being widely utilized by various industries not only for its superior properties, but also its low cost. From the previous studies it is observed that by adding Nano fillers with little amount to base epoxy, electrical breakdown of that material increased. So here testing how the remaining characteristics like permittivity, tensile strength, surface roughness, charge decay characteristics will change by adding micro and Nano fillers to base epoxy resin.

ACKNOWLEDGEMENTS

It gives me great pleasure to express my sincere and heartfelt gratitude to Dr .R.Sarathi for his excellent guidance, motivation and constant support throughout my project. I consider myself extremely fortunate to have had a chance to work under his supervision. In spite of his hectic schedule he was always approachable and took his time off to discuss problems and give his advice and encouragement. I am also grateful for the laboratory facilities provided by him in the High Voltage Laboratory which facilitated my work.

I thank to Mr.Takahiro Imai , TOSHIBA , for providing all composite samples in desired dimensions. I am very thankful to Professors in Physics, Aerospace, Mechanical departments in IITM, allowed to do experiments in their Labs. I thank Mr. Chadrashekar and Mr. Divakar for their help in arranging the equipment setup. I also thank Central work shop department staff for their help in cutting the samples.

My appreciation to my fellow students in the High voltage Laboratory, especially Palash and Animesh for spending their invaluable time with me, while doing the experiments . I would also extend my thanks to Prem, Sahitya, Swathi, Bishal, Sowmmya, Aswin, Chandrika and Gopinath for their support during my work.

This work could not have come to this stage without the support and encouragement from my family and my friends. My heartfelt thanks to all of them.

INDEX

Abstract ii
Acknowledgement iii
List of figures V

1) Introduction 1
1.1. General 1
1.2. A Comprehensive Review of current literature 2
1.3. Objectives of the present study 6
1.4. Scope of the present study 6

2) Experimental studies 8
2.1. Experimental setup 8
2.2. High voltage AC source 8
2.3. UHF measurements 8
2.4. Surface charge measurements 10
2.5. Mechanical test 12
2.6. Dielectric measurements 12
2.7. Understanding the surface condition of epoxy nano composites Due to water aging 13
2.8. Corona inception voltage experimental setup 14
2.9. Static contact angle measurements 15
2.10. Calculation of diffusion coefficient 16

3) Results and discussions 17
3.1. Water absorption characteristics 17
3.2. Permittivity and tan delta experimental results 18
3.3. Surface charge decay characteristics 22
3.4. Surface charge inception voltage with water droplet 24
3.5. Surface charge inception voltage of micro and nano composites With different conductivities of water droplet 26
3.6. Surface roughness of micro and nano composites of epoxy 29
3.7. Analysis of discharges using optical emission spectroscopy of micro And nano composites 32
3.8. Tensile and flexural strength of epoxy micro and nano composites 33

4) Conclusion 37

Bibliography 38

List of Figures

2.1	Frequency Response Of UHF Sensor	9
2.2	Experimental Setup For Surface Charge Measurement	10
2.3	Sample Dimension For Tensile Test	12
2.6	Experimental Setup For Surface Charge Inception Voltage Measurement	14
2.7	Contact Angle Measurement Setup	15
3.1	Water Absorption Characteristics	17
3.2	Characteristic Change In Permittivity With Respect Frequency At 50 Degree Centigrade	19
3.3	Characteristic Change In Permittivity With Respect Frequency At 90 Degree Centigrade	20
3.4	Change In Tan Delta With Respect Frequency At 50 Degree Centigrade	21
3.5	Change In Tan Delta With Respect Frequency At 90 Degree Centigrade	21
3.6	Surface Charge Decay Characteristics For AC Voltage	22
3.7	Surface Charge Decay Characteristics For DC Voltage	23
3.8	Surface Charge Decay Characteristics Of Micro And Nano Composites Before And After Carona Aging	23
3.9	Discharge Inception Pattern In Oscilloscope	25
3.10	Frequency Domain Analysis Of Inception Voltage	25
3.11	CIV For Samples B, D For Different Conductivities Of Water Droplet	27
3.12	Weibull Distribution Plots Of CIV Under Positive DC	27
3.13	Weibull Distribution Plots Of CIV Under Negative DC	28
3.14	Spectrum Analysis Of Sample B	28
3.15	Spectrum Analysis Of Sample D	28
3.16	Discharge Magnitude Comparison Of Micro And Nano Composites	28
3.17	Pictures Of Samples B,D After Degradation With Different Conductivities	30
3.18	3D Images Of Surface Roughness For Sample B With 2500 Us/Cm NH4CL Solution	30
3.19	3D Images Of Surface Roughness For Sample D With 2500 Us/Cm NH4CL Solution	30
3.20	Surface Roughness Characteristics Of Sample B,D For Different Conductivities	31
3.21	Optical Spectroscopy Captured During Arcing On Sample B	32
3.22	Optical Spectroscopy Captured During Arcing On Sample D	32
3.23	Local Plasma Electron Temperature Generated While Arcing	33
3.24	Tensile Strength Characteristic Graph Of Epoxy Composites	34
3.25	Tensile Strength Of Epoxy Composites	34
3.26	Tensile Strain Of Epoxy Composites	34
3.27	Flexural Strength Characteristics Of Epoxy Composites	35

Abbreviations

Dc	Direct current
Uhf	Ultra high frequency
Hfct	High frequency current transformer
Oes	Optical emission spectroscopy
Fdds	Frequency domain dielectric spectroscopy

CHAPTER 1

INTRODUCTION

1.1. GENERAL

Polymer nanocomposites are emerging as a new class of materials for its demanding applications as insulating material in power equipment. ***Nanocomposites*** are named when the disperse phase particle size is less than 100 nm. Based on dimension of the particle, it is classified as 1D (clay layer), 2D (nano tubes) and 3D (fused silica) material. Reinforcement of polymeric resin with nano fillers has resulted in lightweight materials with increased modules and strength, decreased permeability, less shrinkage and increased heat resistance .

In general, the epoxy resin is an indispensable material for insulation systems in power equipment like dry type transformers and rotating machines (kojima *et al.* 1993b). The epoxy resin is used not only as insulating material but also as structural material because the material is cost-effective. In addition, to use the insulating material for out-door purposes, it is essential to understand the tracking phenomena of the epoxy nanocomposite material. Also it is essential to understand the characteristic variation that occurs discharge as well as the discharge initiated due to water droplet under AC and DC voltages. Also use of optical emission spectroscopy for identification of characteristic changes that occurs to insulating material during tracking forms important study in the recent times.

In Insulation structures, incipient discharges often precede arcing and can cause severe damage to insulation of the power equipment (T. Tanaka *et al. 2008*). The generated incipient/partial discharge current pulses are with rise and fall times of

few nano seconds, signals of Ultra High Frequency (UHF) range, (300-3000MHz) are excited (M. Kozako *et al. 2004*) . The UHF technique for PD identification in power equipment is giving acceptance due to its high sensitivity and good signal to noise ratio(B. Deneve *et al. 1993*) . Thus use of UHF technique for identification of incipient discharges especially generated due to a water droplet, under AC and DC voltages, the results are scanty and hence considerable database has to be generated.

1.2. A COMPREHENSIVE REVIEW OF CURRENT LITERATURE

Polymer/clay nanocomposites have a long history of development. The progress of development has been reported since the nineteen sixties. Toyota R & D group, Japan first synthesized Polymer clay nanocomposites in 1992 consisting of nylon as base matrix material and the nanoclay as the reinforcement filler. They have reported thermal [mass loss, decomposition], mechanical [strength, modulus, toughness] and physical [barrier, permeability and optical] properties are increased over pure nylon matrix (Usuki *et al*. 1993a; Usuki *et al*. 1993b; Kojima *et al*. 1993a; Kojima *et al*. 1993b). They have shown 40% higher tensile strength, 68% higher tensile modulus, 60% higher flexure strength than pure nylon matrix polymer. In addition to this, they observed an increase of HDT from 65°C to 152°C.

Nanocomposites, made up of epoxies and inorganic materials, have been a vital subject of research not only because epoxies are one of the most important type of thermosetting resins, widely used as electrical insulation material, surface coatings, adhesives, castings and laminates, but also due to its unique properties rendered by distinctive size, surface chemistry and topology (Aijuan and Guozheng, 2003).

Takahiro Imai *et al.,* (2002) studied the characteristics of epoxy-silicate nanocomposites prepared by dispersing synthetic layered silicates modified with alkyl-ammonium ions. They observed that glass transition temperature of the epoxy nanocomposites is high compared to pure epoxy. They also concluded that the relative permittivity and dielectric loss of epoxy nanocomposites increases with temperature.

T.Tanaka et al., (2004) carried out extensive study in the area of nanocomposites. They have concluded that addition of small amounts of nanometer size fillers to the polymer enhances the thermal, electrical and mechanical properties of polymer nanocomposites.

J.K.Nelson and Y Hu (2005) studied the incorporation of nano and micro particles into thermosetting resins. They have concluded that the breakdown time due to electrical stress is higher in nanocomposites compared to micro composites material. They observed that the dielectric loss of the material is less in nanocomposites compared to micro filler added composites, irrespective of frequency of the applied voltage.

Takahiro Imai *et al.,* (2006b) studied effects nano and micro filler mixture on electrical insulation properties of epoxy based composites. They have observed during continuous voltage rising test, the filler mixture composites having more electrical breakdown strength than conventional filled epoxy. But under application of constant voltage, the filler mixture having more insulation breakdown time compared to neat epoxy.

Masahiro Kozako et al., (2005) studied the electrical and mechanical properties of epoxy/alumina nanocomposites. They concluded that the electrical breakdown time is high in nanocomposites compared to pure epoxy. They also observed the flexural strength is high in nanocomposites compare to pure epoxy.

Takahiro Imai *et al.,* (2006c) studied the electrical properties of epoxy nanocomposites with homogeneous field and non-homogeneous field condition. They have concluded the electrical breakdown strength of nanocomposites is higher in non-homogenous field as compared to homogenous field. In addition to this, the failure time under electrical stress is high in nanocomposites unlike in pure epoxy.

Takahiro Imai *et al.,* (2006a) studied the effect of temperature on the mechanical and electrical properties of epoxy-layered silicate nanocomposites. They have reported that the volume resistivity of nanocomposite is gradually decreases with increase in temperature. They also mentioned that, the relative permittivity and electrical breakdown time of nanocomposites increases with temperature.

Gonon et al., (2005) studied the effect of water absorption on dielectric constant, dielectric loss and resistivity of epoxy composites. They have concluded the dielectric constant and dielectric loss is increased due to water ageing. The resistivity of the material drastically got reduced due to water absorption.

Fukuda et al., (1997) reported an impact of water absorption, the dielectric constant and dielectric loss of cycloaliphatic epoxy resin with silica powders increases. But without silica powders with epoxy resin, the values of dielectric constant and dielectric loss are reduced with increase of absorption of water.

Asma Yasmin et al., (2003) studied the mechanical properties of epoxy nanocomposites. They have observed that there is no improvement in the tensile strength of nanocomposites compared to pure epoxy. But there is increasing elastic modulus of nanocomposites compared to pure epoxy.

Soo-Jin Park *et al*., (2002) studied thermal property of [decomposition, mass loss] epoxy-clay nanocomposites, and observed that weight loss is less in nanocomposites compared to epoxy resin.

Masahiro Kozako et al., (2006) studied electrical, mechanical and thermal properties of epoxy/alumina nanocomposites. They have reported electrical breakdown time, PD resistance and flexural strength increases in epoxy/alumina nanocomposites as compared to neat epoxy. In addition to this, they have concluded that a relative permittivity of epoxy nanocomposites is more compare to pure epoxy. There is no change in glass transition temperature between nanocomposites and pure epoxy.

The reason behind changing in characteristics mainly Increase in surface area of nano particle, which alters polymer behaviour Changes in permittivity value Changes in space charge distribution in the insulation structure .Also because of high packing density, the accumulated charge is reduced on its surface area (A. Yasmin et al. 2003). When the material is packed with nano materials, the filler acts as scattering site. The eletrons injected from the high voltage electrode in solid insulation .Due to dispersed nano particles , the elctrons transfer the energy to the nano particles and lose of momentum involving in reaction. Since the particles are so closely packed, the electrons cannot gain momentum to involve in the process of breakdown. For the cause of damage to the insulation , it requires additional voltage to cause any catastrophic failure of insulation.

Samples tested here are , first one Wallastonite molecular formula is CaSiO3 and its theoretical composition consists of 48.28% CaO and 51.72% SiO2 and the second one silica formula SiO2.

1.3. OBJECTIVES OF THE PRESENT STUDY

The following aspects are the important objectives of the present study

(i) To understand the diffusion coefficient of epoxy nanocomposites (ii) To understand the characteristic variation in permittivity and tan δ of epoxy nanocomposites at different frequency and temperature. (iii) To understand the charge decay behaviour of epoxy nanocomposites under AC and DC voltages. (iv) To understand the characteristic variation corona inception voltage of water droplet on epoxy nanocomposites and with micro composite materials, under AC and DC voltages and understand the characteristics of UHF signals generated due to a water droplet (on epoxy nanocomposites) initiated corona and at the time of arcing, under DC voltages, by use of broadband sensors. (v) to understand the variation of corona inception voltage of micro and nanocomposites by changing the conductivity of water droplet from 500 μs/cm to 2500 μs/cm under AC and DC (vi) to understand the surface roughness of micro and nanocomposites with different conductivities of water droplet (vii) To understand the optical emission characteristics during water droplet initiated discharges.(vii) To understand certain mechanical properties of material especially the tensile strength and the flexural strength of the epoxy nanocomposites.

1.4. SCOPE OF THE PRESENT STUDY

The thesis is structured to preserve a cogency of the reported results. . It comprises of four chapters.

The first chapter introduces the topic on epoxy nanocomposites, the need for taking up the present investigation is explained at length. A survey of current literature broadly covering the subject is reported as completely as possible. After obtaining panoramic

view on the topic through literature survey, the objective of the present study was highlighted.

The second chapter is mainly devoted to experimental study The details of experimental studies carried out to understand the electrical, and mechanical properties of the materials are also detailed.

The third chapter, results obtained based on the experimental study were provided and analyzed by discussing the results obtained by other researchers on the topic, to arrive at reasonable conclusions.

The chapter four presents a summary of the author's contributions to the subject on understanding the materials properties of epoxy nanocomposites.

CHAPTER-2

EXPERIMENTAL STUDIES

2.1. EXPERIMENTAL SETUP

The experimental setup for understanding the surface discharge and corona discharge activity of different test samples under AC voltages is shown in Figure 2.6. The experimental setup includes the High voltage source, UHF measurements, surface charge measurement and dielectric measurement, tensile and flexural strength measurement.

2.2. High voltage AC source

A 100 kV, 5 kVA, 50 Hz test transformer is used for generating high AC voltage. The voltage was increased to the required level, at a rate of 300 V/s. The required AC/harmonic AC voltage with different THD's wave shapes are generated by using function generator (Agilent 33250A). The output of the function generator is connected to Trek amplifier (Model 20/20C). The high voltage probe (Tektronix model. No. P6015A) was used to measure the required AC/harmonic AC voltages.

2.3. UHF Measurements

The partial discharge in the transformer due to the different discharge sources is implemented using Ultra High Frequency sensor. Proper sensor/detector is used to analyse the signals form the discharge source. The requirements of the UHF sensor is as follows,

(1) The sensor should be designed for a predefined frequency band and should be able to acquire the signals in that band.

(2) Need to ensure that disturbance caused due to insulation breakdown, mobiles should be neglected and detector should have high sensitivity to the partial discharge signals.

(3) Make sure that the sensor functionality is not impacted due to internal field configuration of power apparatus to which it is connected.

The characteristic frequency content of the signals from the different discharge sources varies and hence the detector should have a broadband response.

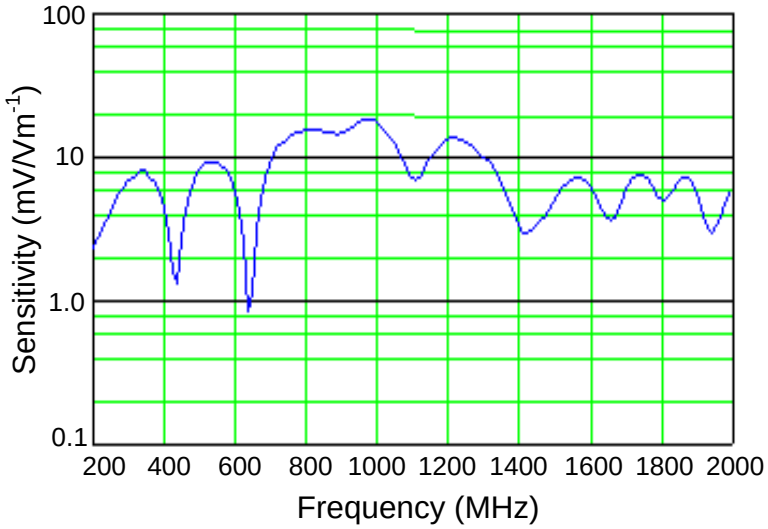

Figure 2.1. Frequency Response of the UHF sensor

The sensor used in the present study is a broadband UHF sensor which is placed at a distance of 20cm away from the test cell to avoid any discharge from the test cell to the sensor. The sensitivity response of the broadband sensor is shown in Figure 2.1 (Judd *et al*., 1998b). The output of the UHF sensor is connected to the high bandwidth digital storage oscilloscope (LeCroy four channel digital real time oscilloscope, 3 GHz bandwidth, operated at 20 GSa/s) with input impedance of 50 ohms and to spectrum

analyser. The HFCT sensor (ETS LINDGREN Model 94111-1) was used to measure the injected discharge current pulses.

2.4. Surface Charge Measurement

In the present study, the surface charge decay characteristics of epoxy nanocomposite and micro composite material before and after corona charging process were analyzed through Electrostatic Voltmeter. Different methodologies were adopted in the past studies to examine the processes by which free charges can be generated and accumulated on insulation surfaces. These studies have included the use of a sharp-pointed emitter (Cooke 1982), corona discharges on the high-voltage electrode (Giacometti *et al*., 1992), and an external corona source (Kumara *et al*., 2012), for surface charge production. Figure 2.9 shows experimental setup for surface charge measurement studies.

A needle-plane electrode configuration was used for corona generation. The needle was connected to high voltage and the sample surface to which the charge has to be deposited is

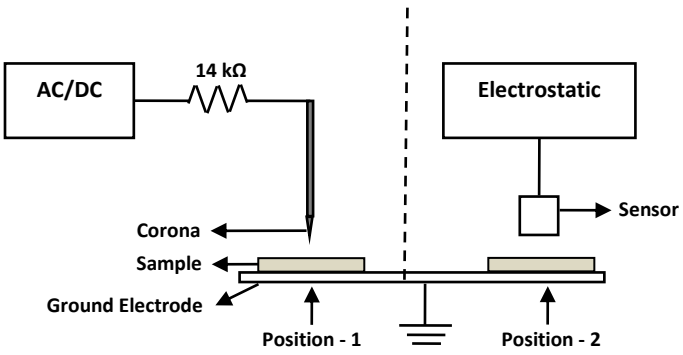

Figure 2.2. Experimental setup for surface charge measurement

Placed on the bottom ground electrode. The supply voltage for generating corona activity was carried out by maintaining the voltage at 8 kV (AC/DC voltage) for 3 minutes. The required AC/DC voltages for the study were generated by using Trek amplifier (Model 20/20C) by providing required wave shape as input from function generator (Agilent 33250A). After specific time duration of charge spraying by corona discharge process, the surface charge was measured (position-2) through Electrostatic Voltmeter (Trek Model 341B). The gap distance between the sensor and the test specimen was maintained at 2mm which could cover charge measurement up to a radius of 5mm on the surface of the specimen. The surface charge measurement involves two stages. In the first stage the charge is deposited (referred as position-1) by corona discharge process. After a predetermined time period, the sample is moved on the same platform and surface charge is measured using electrostatic voltmeter (referred as position 2). The charge (Q) on the surface of the oil impregnated pressboard is calculated as,

$$Q = V \frac{\in_o \in_r A}{d}$$

where, ε_o electric permittivity of vacuum, ε_r is the relative permittivity of the medium, A is the area of cross section of the sensor, d is the distance between sensor and the sample surface and V is the voltage measured by Electrostatic Voltmeter. A minimum of three samples were used, for every experimental study, to ascertain the characteristics of the material.

2.5. Mechanical test

Tensile and Flexural Test

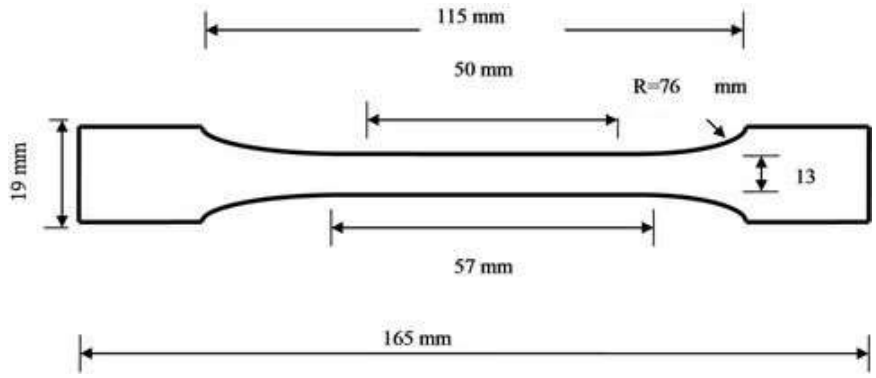

Fig 2.3. Sample dimensions for Tensile test

Tensile strength test is carried out to understand the ability of a material to resist breaking under tensile stress. The breaking load and the elongation at break were measured and the tensile stress computed. In general, the ability of a material to resist deformation under a load is its flexural strength. For materials that do not break, the load at yield, typically measured at 5% deformation/strain of the outer surface, is the flexural strength or flexural yield strength. This test was carried out using universal testing machine (Instron 4301 of 500 kg capacity). The pulling speed during the test was maintained at 3mm/min.

2.6. Dielectric Measurements

Frequency Domain Dielectric Spectroscopy (FDDS) measurements were carried out to understand the fundamental dielectric properties of the material at different

frequencies at different temperatures by using Novo control technology broadband dielectric/impedance spectrometer (Alpha-A High performance frequency analyser). Its frequency range is from 3μHz – 40 MHz, the test temperature range can be from -10°C to 500°C. In the present study, the dielectric response studies were carried out in the frequency range of 10Hz to 10^6Hz investigated at 30, 50, 70and 90^{o}C. The test electrode diameter of 20mm is used for pressboard sample. The AC sinusoidal voltage of 1V (RMS) is applied to test sample. Based on the measured voltage, current and their phase differences parameters such as real and imaginary permittivity, dielectric loss (dissipation factor) tan (δ) etc. were measured. The constant moisture equilibrium and temperature are maintained by keeping the electrode in a sealed vessel enclosed in the equipment. The FDS measurement was carried out with epoxy nanocomposites.

2.7. Understanding the surface condition of epoxy nanocomposites due to water ageing

The essential characteristics of an insulating material is to have surface hydrophobic. This characteristics is important to avoid any leakage current through surface causing tracking followed with flashover, during operation. Hence, a methodical experimental study was carried out by ageing the specimen in water to realize the hydrophobic characteristics and the diffusion characteristics of water in insulating material.

The aging was carried out by placing the epoxy nanocomposite specimen cut is square piece of 3cmx3cmx1mm and immersed in a distilled water bath maintained at different temperatures viz. 30, 60 and 90°C. The mass of each sample was measured to note the change in weight with time, during aging, to calculate the diffusion coefficient of the

material. The hydrophobic characteristics of epoxy nanocomposites were measured through contact angles measurement. The aged specimens were then placed in the normal atmosphere and characteristic variations in the contact angle during the drying process were observed. The characteristic changes in the surface of the material due to water ageing analysed through contact angle measurement and by Atomic Force Microscopy (AFM).

2.8. CORONA INCEPTION VOLTAGE EXPERIMENTAL SETUP

In transmission distribution limes, the water droplets can be formed on the insulator surface due to rain or condensation of fog causing local electric field intensification near to it there by causing inception of corona followed by surface charge activity (R. Sarathi et al) . If the electric field intensity is high due to water droplet, corona discharge can occur from edges of the water droplet leading to reduction in hydrophobicity of the material, arcing leading to carbonization of surface and finally bridging of electrode gap leading to catastrophic failure of insulation structure. Conductivity of rainy water or dew may vary so experiment was carried out for different conductivity of water droplets.

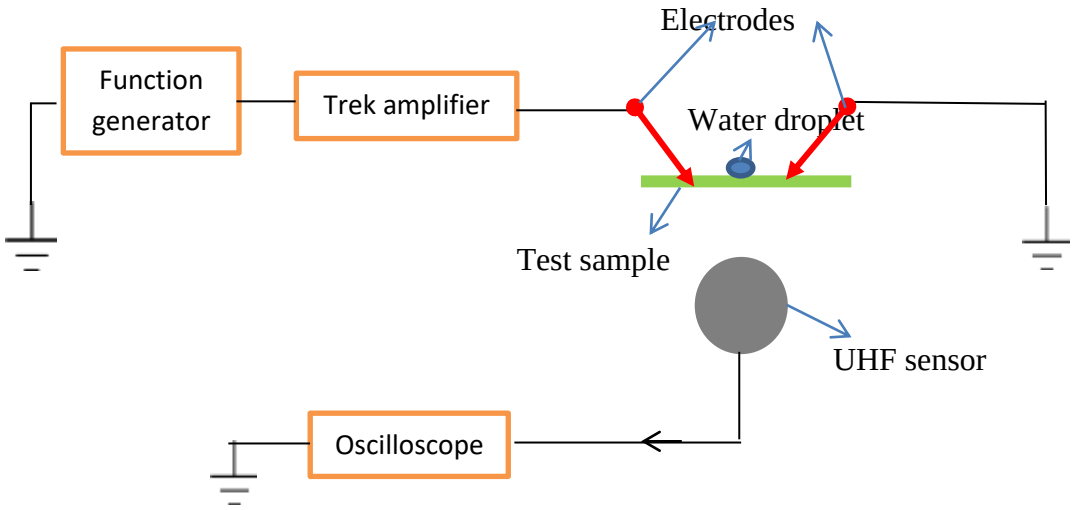

Figure 2.6. Experiment setup for surface charge inception voltage measurement

2.9. STATIC CONTACT ANGLE MEASUREMENT

It has been shown that the measure of contact angle of a water droplet is an indirect measure of hydrophobicity of the material (T.Tokoro *et al*., 1999). The contact angle (θ) depends on the surface energy of the material. Figure 2.4 gives details about the contact angle and the method of measuring it. In the present work, the static contact angle was measured by liquid droplet method, using distilled water, assuming constant radius of curvature and thereby determining contact angle from the measurement of height and base diameter for a known volume (Wang *et al*., 1999). The size of the drop was about 1.5mm in diameter. The contact angle was measured using the following equation,

$$\theta = 2\tan^{-1}\left(\frac{2h}{d}\right)$$

where d is the diameter of the liquid drop and h is the height of the liquid drop. After the solution was placed over the surface of the specimen, the contact angle was measured within 5 seconds. For each specimen, the contact angle was measured at six different locations and average of it was considered as the contact angle.

2.10. CALCULATION OF DIFFUSION COEFFICIENT

The following one dimensional diffusion equation can be used to understand the water diffusion in the plate samples,

$$\frac{dc}{dt} = D\left(\frac{d^2c}{dx^2}\right) \tag{2.2}$$

where c is the water content in the polymer, t is the duration of soaking, D is the diffusion coefficient and x is the depth of moisture penetration, generally unknown.

The diffusion coefficient for volume penetration of distilled water into HDPE and SR was determined at different temperatures. Crank (1975) developed the relationship, which indicates level of saturation in absorption of liquid into the material. When diffusion is driven by the concentration gradient and if there is no chemical change between liquid and material, this would result in mass change and the rate of absorption will be initially linear with $t^{0.5}$, where 't' is the time of absorption. Hence,

$$\frac{\Delta m(t)}{\Delta m_{\infty}} = 2\sqrt{\frac{Dt}{l^2}}\left\{\sqrt{\frac{1}{\pi}} + 2\sum_{n=1}^{\infty}\left[(-1)^n \cdot \text{ierfc}\left(\frac{nl}{2\sqrt{Dt}}\right)\right]\right\}$$

where D is the diffusion coefficient , l is the thickness of sheet , n is the number of sheets , 'ierfc' is the integrated complimentary error function, $\Delta m(t) = m(t) - m(0)$ and $\Delta m_{\infty} = m_{\infty} - m(0)$. In this, m(t) is mass at time 't', m(0) and m_{∞} are initial mass (at time t=0) and after infinite time respectively. Crank (1975) formulated the final expression to calculate diffusion coefficient and if the linear dependency in plot $\Delta m(t)/\Delta m(\infty)$ vs $t^{0.5}$ is not observed, then the diffusion constant is obtained by equating $\Delta m(t)/\Delta m_{\infty}=0.5$. Simplifying the equation we get,

$$D = \frac{\pi L_{0.5}^2}{64 t_{0.5}}$$

where L is thickness of the specimen. t is the time at which the % weight value at half the peak in characteristic graph between % wt Vs. time.

CHAPTER-3

RESULTS AND DISCUSSION

3.1. WATER ABSORPTION CHARACTERISTICS

Fig. 3.1. Shows characteristic variation weight gain of epoxy nanocomposites with time during water ageing. It is observed that the water gets diffused into epoxy nanocomposites and gets saturated. It is clear that filler material play a major role on level of water absorption during water immersion test. In general, it is observed that, irrespective of type of filler included, the saturation level is reached in about 1200 hours of ageing.

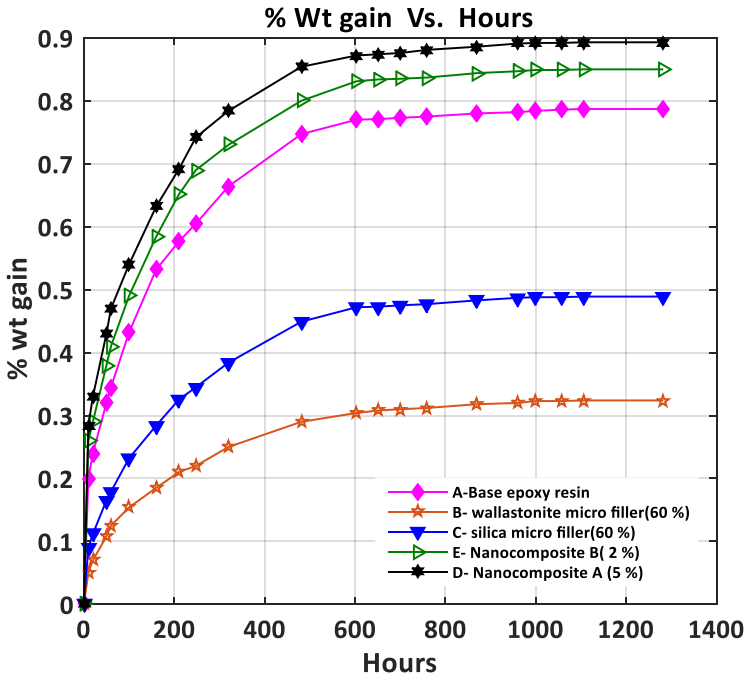

Figure 3.1. Water absorption characteristics (all samples)

Based on the theory explained in Chapter-2, for calculation of diffusion coefficient, the calculated diffusion coefficient of the material is provided in Table-1. It is realised that water absorption is high with nanocomposites than the nano micro composites. By adding 5% Nano fillers, composite absorbing more and more water than 2% Nano composite and also base epoxy resin, diffusion coefficient increased. By adding 60 % fused micro filler, water absorption levels decreasing, diffusion coefficient decreased. By increasing the Nano filler content in pure epoxy, quantity of water absorbing by the composite material increasing

Table 3.1. Diffusion coefficient of epoxy composits

S.No	Material	Diffusion coefficient (m^2/sec)
1	A- Base epoxy resin	4.15×10^{14}
2	C- Epoxy with 60% silica micro filler	2.99×10^{14}
3	B- Epoxy 60% wallastonite micro filler	2.93×10^{14}
4	E- Epoxy with 2 % Nano filler	5.01×10^{14}
5	D- Epoxy with 5 % silica Nano filler	6.31×10^{14}

3.2. PERMITTIVITY AND TAN DELTA EXPERIMENTAL RESULTS

In figures 3.2,3.3 , the characteristic change in permittivity of epoxy nano and micro composite samples with respect frequency has shown and in figure 3.4,3.5, the characteristic change in loss tangent of epoxy composites with respect frequency has shown. From the figure 3.4, it is clearly observed that nanocomposite

material with 5 % weight is showing less permittivity than base epoxy and micro composite material. For all samples , permittivity decreasing correspondingly with respect increasing frequency.

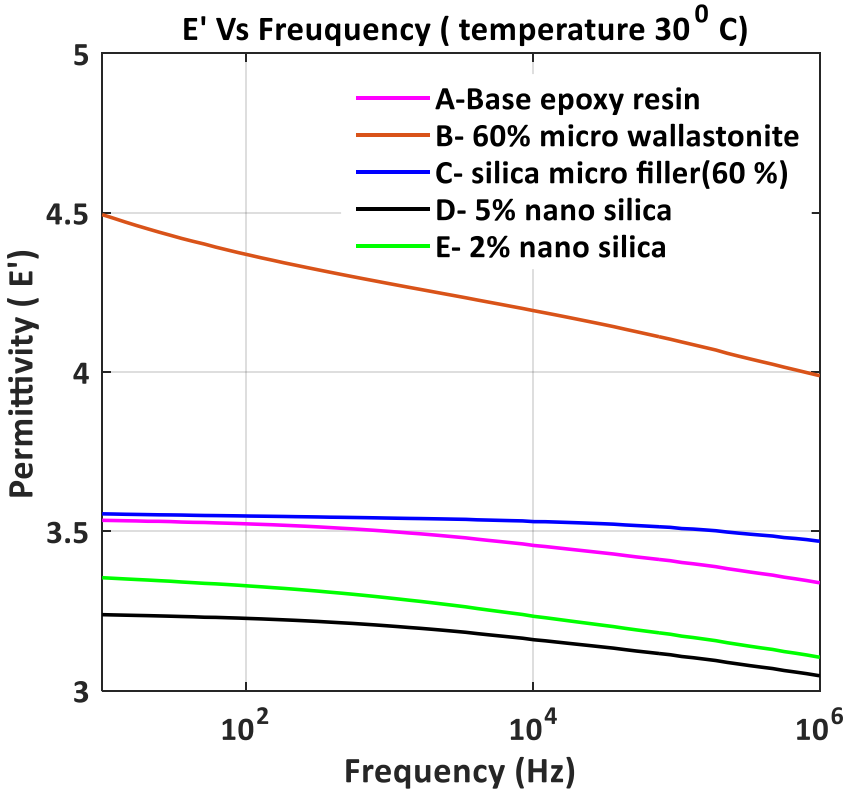

Figure 3.2. Characteristic change in Permittivity with respect frequency (at 50^0C)

At room temperature, 60% fused silica micro composite material (sample C) has same value of ε' as base epoxy but sample C shows stable value of ε' independent of frequency . 60 % wallastonite micro filler composite (sample B) has higher value of ε' than the remaining samples but this material (sample B) is frequency dependent , the value of ε' decreasing drastically by increasing frequency. By increasing nano filler content in pure epoxy , permittivity value decreasing. With respect temperature, the value of ε' in micro filler composites are increased that means micro composite

material are temperature dependent but nano composite material are independent of frequency and also temperature.

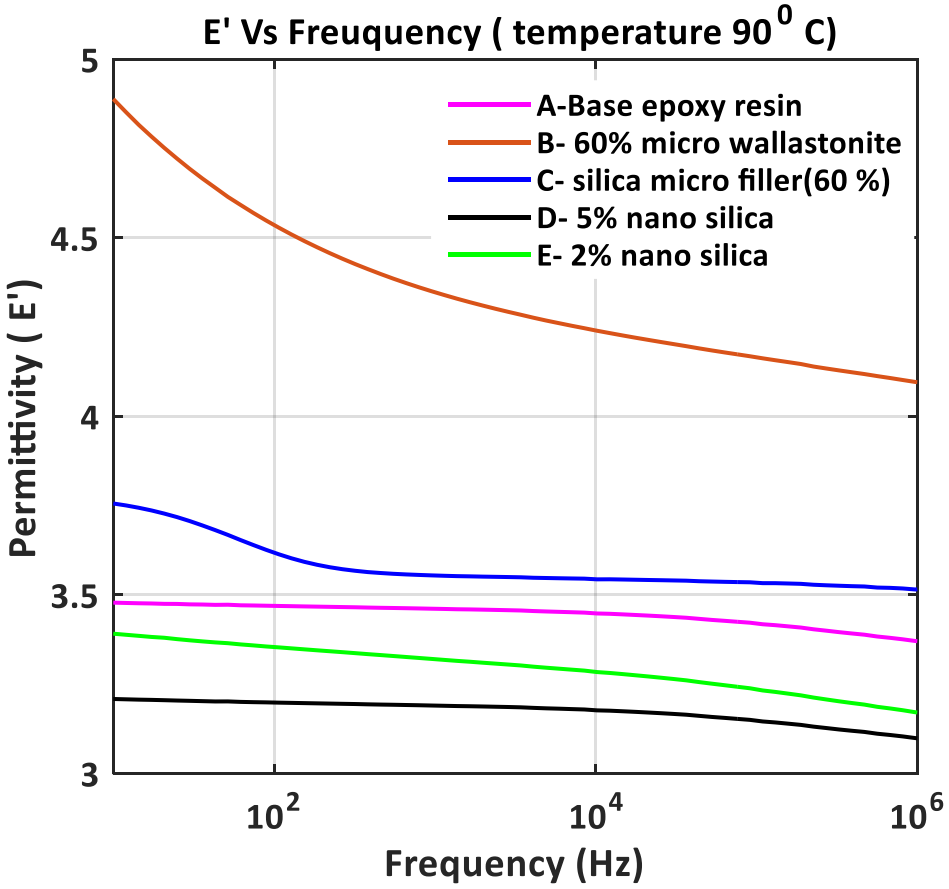

Figure 3.3. Characteristic change in Permittivity with respect frequency (at 90^0C)

From the figure 3.5, if temperature increase then loss tangent (Tan δ) value also increasing in all 5 samples but increment in sample B (60% wallastonite micro filler) high . Base epoxy and nano filler composite material have increment in Tan δ value with respect frequency. From figure it is clearly showing that loss tangent value is fluctuating in sample C (60% fused silica micro filler) with respect frequency and also temperature dependent.

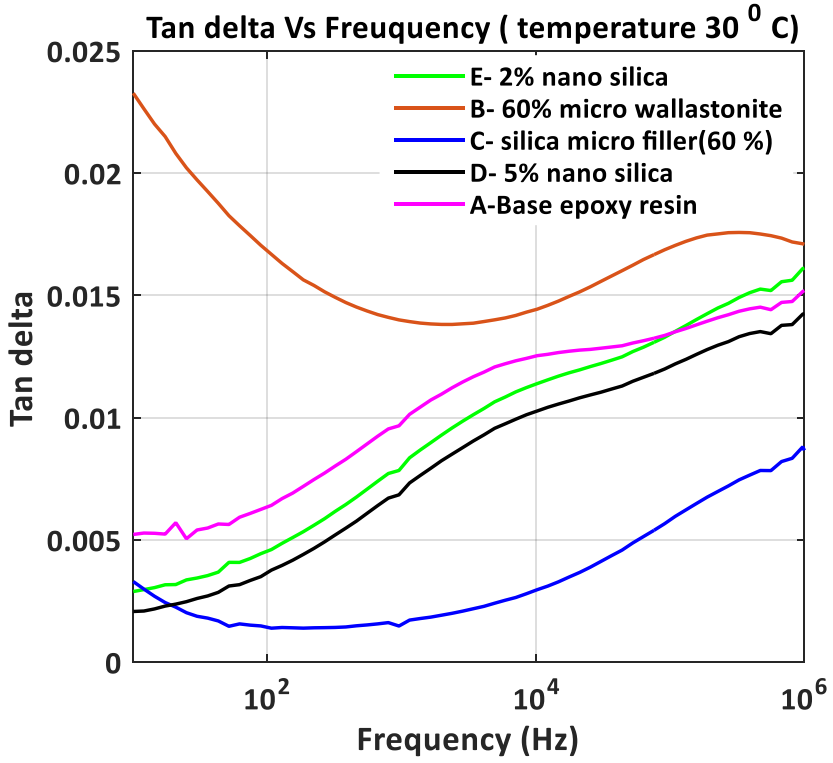

Figure 3.4. Change in Tanδ with respect Frequency (at 50^0C)

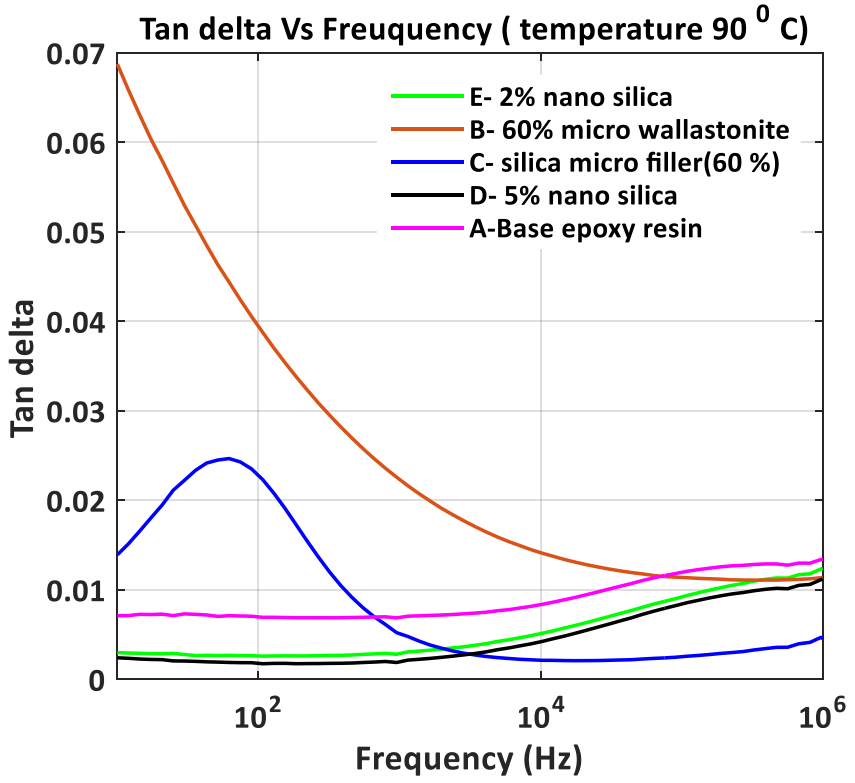

Figure 3.5. Change in Tanδ with respect Frequency (at 50^0C and 90^0 C)

3.3. surface charge decay characteristic results

As explained in chapter 2, the experiment was carried out and how much charge accumulating on surface and the rate of decaying of charge is obtained and the results are shown in below figures. In figure 3.6, surface charge decay characteristics of epoxy composites for Alternative voltage of magnitude of 10KV have shown and in figure 3.7, characteristics under DC voltage of magnitude of +10KV and -10 KV have shown. In Figure 3.8., surface charge decay characteristics of micro and nano composite filler before and after corona aging have compared. It indicates that fast charge decay initially occurs with larger part of charges dissipating, which is followed by a progressively slow one. it can be observed that, for 10 KV AC supply, charge accumulated on its surface in micro composites are high than base epoxy and nano filler composites and charge decay rate also slow in micro filler composites.

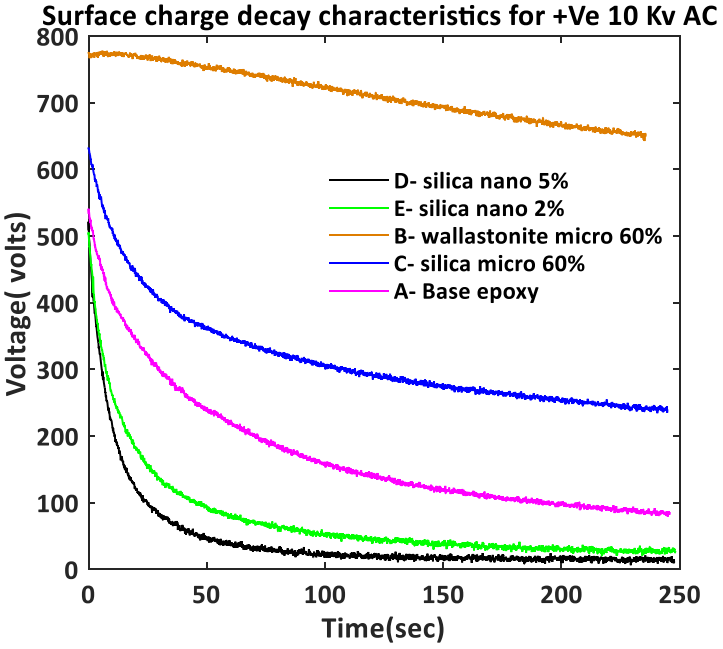

Figure 3.6. Surface charge decay characteristics For AC voltage (10 KV)

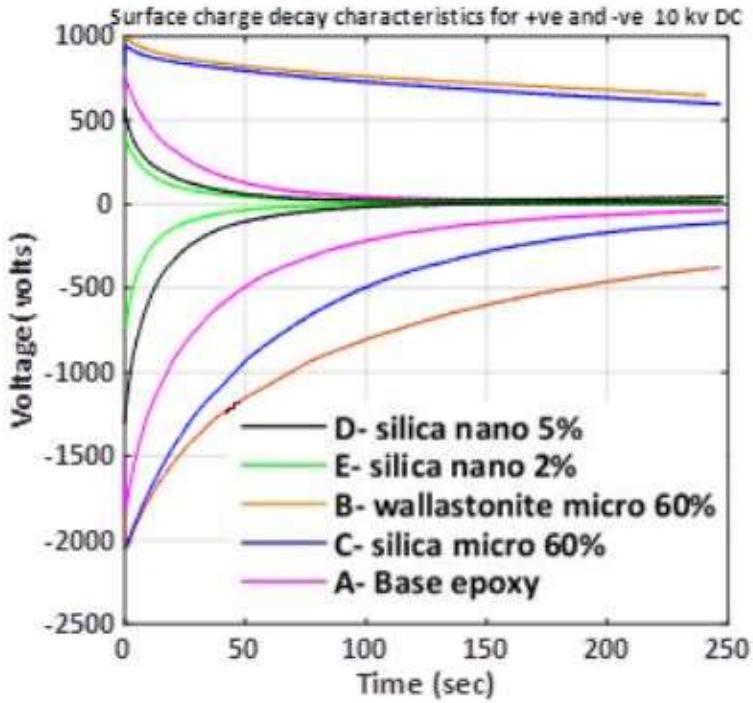

Figure 3.7. Surface charge decay characteristics For DC voltage (+10 KV and -10 KV)

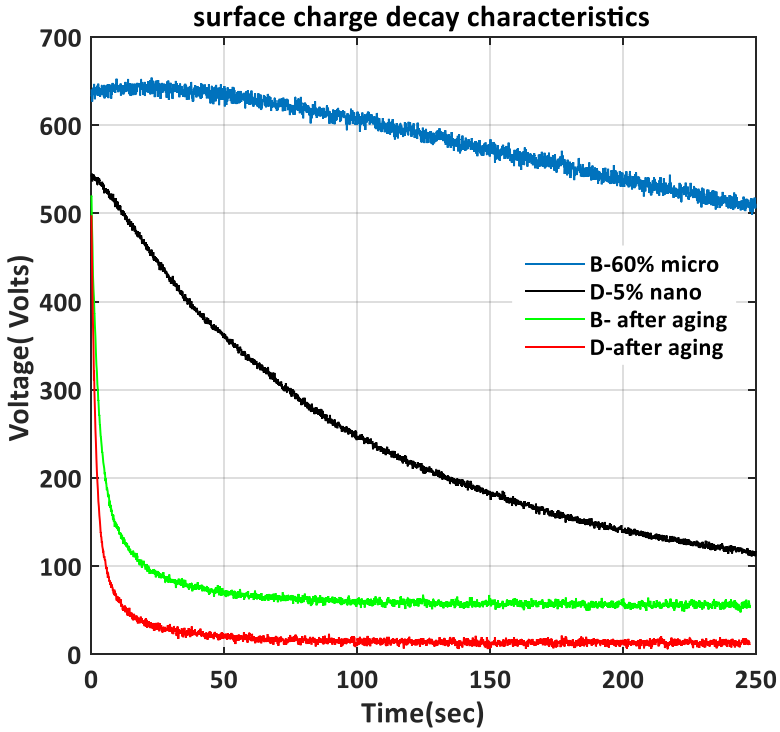

Fig 3.8. Surface charge decay characteristics of micro and nano composite fillers before and after corona aging

60% wallastonite micro composite (sample B) storing more than other samples. From the figure 4.3, for Positive DC and negative DC, all composite material following same pattern as AC supply but for DC voltage, charge accumulation on surface is more. When compare with positive DC and negative DC, charge accumulating is high in Negate DC. From the figure 4.8 , After corona aging (high frequency and high magnitude 20 KV AC supply for 10 minutes) , micro and nano filler composites charge decaying rate is high but in nano composite material decaying rate is superior that micro. . With the increase of the radiation dose, the rate of charge decay increases.

3.4. Surface discharge Inception voltage (CIV) with water droplet

As mentioned in chapter 2, the variation in surface charge inception voltage or corona inception voltage (CIV) due to water droplet of different conductivity on epoxy nanocomposites under DC and AC voltages are observed. In figure 3.9, waveform generated in oscilloscope while incepting is taking place and in figure 3.10 , fourier series frequency domain analysis of inception waveform. In table 3.2,3.3,3.4 , inception voltage for 5 different samples shown for AC and +Ve DC and –Ve DC supply.

Surface charge inception voltage (or) corona inception voltage of all samples are high for Negative DC supply less for AC supply. By adding micro fillers (wallastonite or fused silica) inception voltage decreased than base epoxy meanwhile by adding Nano fillers (2% or 5 %) inception voltage increased than base epoxy resin.

Sample type	A	B	C	D	E
CIV (AC 10 kV)	4.54	2.73	4.23	6.30	4.75

Table 3.2 Inception voltage for 10 KV AC supply

Sample type	A	B	C	D	E
CIV (+ve DC 10 kV)	9.63	9.51	8.33	11.35	10.55

Table 3.3. Inception voltage for 10 KV Positive DC supply

Sample type	A	B	C	D	E
CIV (-veDC 10 kV)	-10.9	-8.93	-9.56	-11.8	-11.3

Table 3.4 Inception voltages for 10 KV Negative DC supply

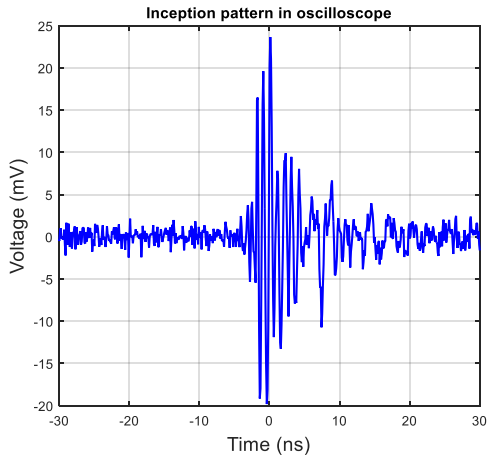

Fig 3.9. Inception pattern in oscilloscope

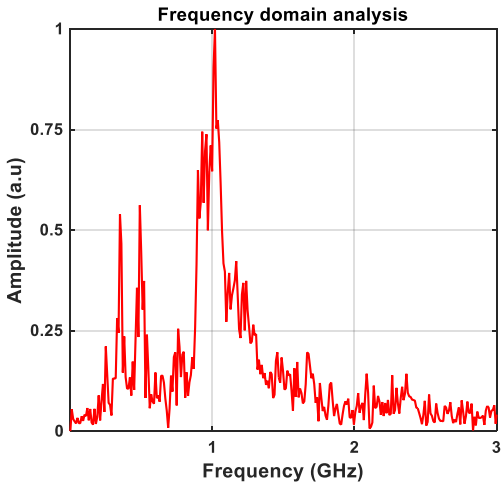

fig 3.10. Frequency domain analysis

Inception voltage value increasing with increase of nano filler percentage in epoxy means inception voltage is high in 5% nano composite (sample D) than 2% nano composite (sample E). Samples following same order for AC and DC supply. Inception is occurring in short duration with rise time few nano seconds. From the figure 3.10, it is observed that dominant frequency was 1GHz in frequency domain analysis of inception wave means at that frequency amplitude of discharge is high.

3.5. Corona inception voltage of micro and nano composites with different conductivities of water droplet

In figure 3.11, corona inception voltage of two samples, 60% micro filler and 5% nano filler composites are compared. Micro filler composite has shown as sample B and nano filler composite has shown as sample D. in figure 3.12 , for differnet conductivies weibull distribution plots of corona inception voltage of sample B and sample D for positive DC supply magnitude of 10KV has shwon . Weibull Plots for Negative DC of these samples has shown in figure 3.13. by connecting the Ultara high frequency (UHF) sensor to Spetrum analyser it is easy to obserberve the discharge magnude when the arcing intiated. From the figure 3.11, corona inception voltage is less for AC suppy and high for Negative DC supply at conductivity of 500 μs/cm. nanocomposite materal's (sample D) inception voltage is high than micro composite material (sample B) for all conductivity water droplets. By incresing the conductivity of water droplet, surface discharge inception voltage (CIV) is decreasing.

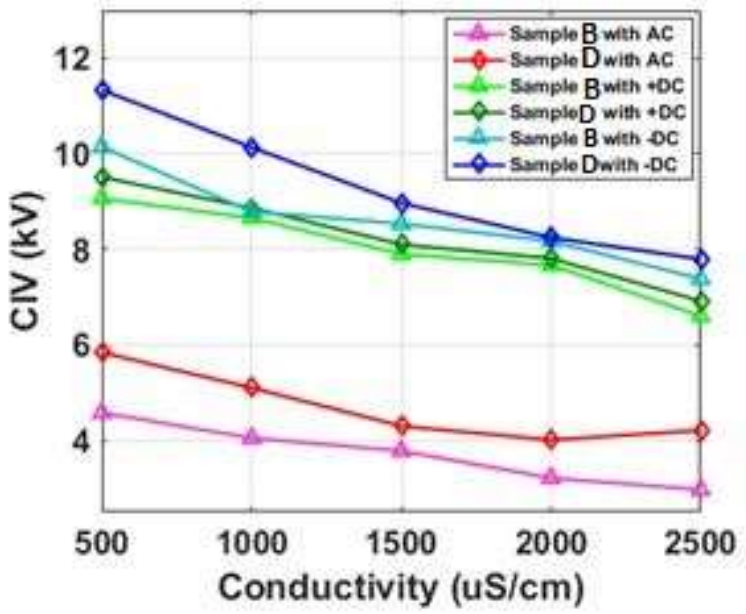

Figure 3.11. CIV for samples B, D for different conductivities of water droplet

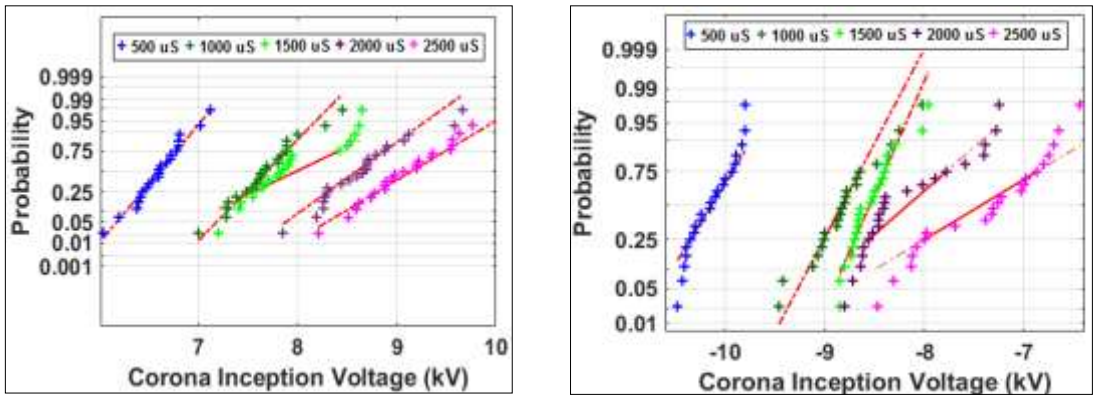

a)Sample B for +Ve Dc (10KV) **b) Sample D for +Ve Dc (10KV)**

Figure 3.12. Weibull distribution plots of CIV under positive DC

In figure 3.14, spectrum analyser plots has shown of sample B and in figur 3.15, plots of Sample D has shown and in figure 3.16, these two samples are compared.

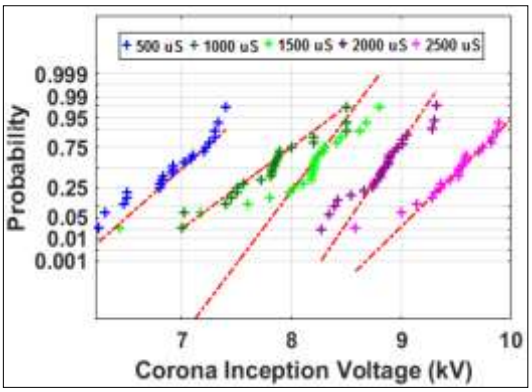

a) Sample B for -Ve Dc (10KV)

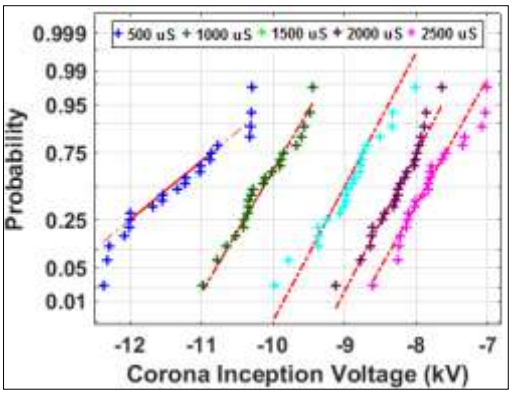

b) Sample D for -Ve Dc (10KV)

Figure 3.13. Weibull distribution plots of CIV under negative DC

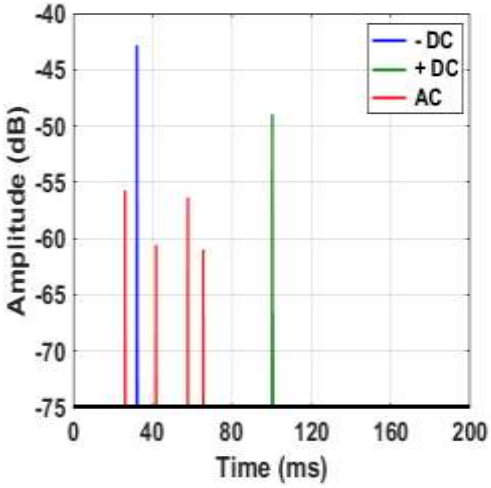

Figure 3.14. Spectrum analysis of Sample B

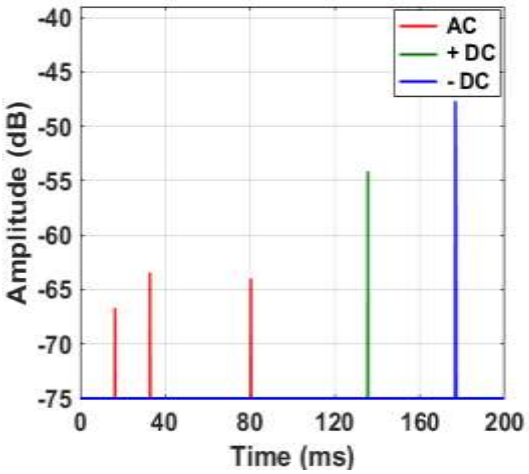

figure. 3.15. Spectrum analysis of Sample D

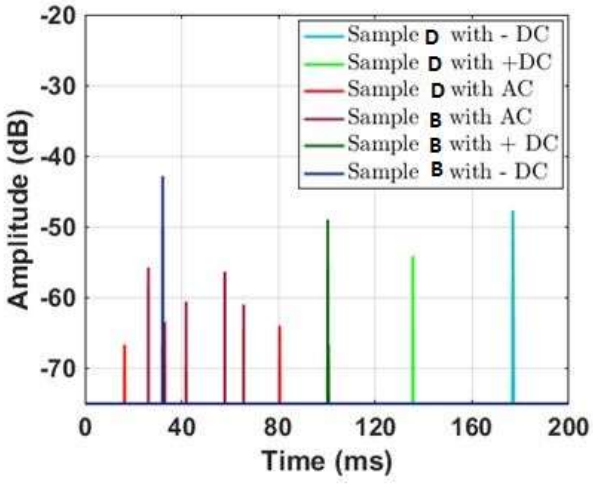

Figure 3.16. Discharge magnitude comparision of micro and nano composites

From the figures 3.12 , for micro composite filler under Positive DC supply, by increasing the conductivity, the slope (shape parameter) of the plot is decreasing means non homogeneity in surface charge inception voltages (CIV) but in nano composite materials slope of the plot is nearly same till the conductivity reaches the value of 1500 μs/cm means homogeneous characteristics . After 1500 μs/cm nano composite material also following non-homogeneity. From the figured 3.13 , under negate DC supply , micro composite materal has nonhomogeneous by increasing the conductivtiy of drop let .But nano compoiste material under Negative DC exibiting homogeneous characterisctics independent of conductivity of water droplet.

Form the figures 3.14,3.15,3.16, under AC supply number of discharges are high at short time in two samples and discharge magnitudes are less in Sample D. under positive DC and negative DC , number of discharges are less but discharge magnitde is high under negative DC supply. Discharge magnitudes are less in Sample D than Sample B under all voltages.

3.6. Surface roughness of micro and Nano composites of epoxy

The insulation material which has high surface roughness will degrade or will damage early and which has less roughness has long life. in figure 3.17,Surface roughness has shown by using camera pictures and 3-D images and also graphical representation. Pictures of samples after degradation had shown, with water droplet different conductivities.

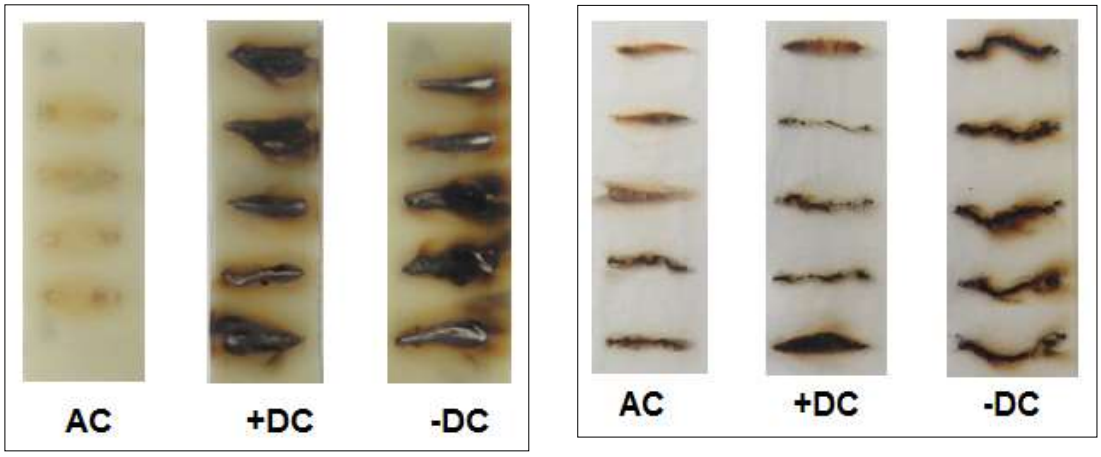

a) Picture of Sample B

b) Pictures of Sample D

Fig. 3.17. Pictures of samples B, D after degradation with different conductivities (500, 1000, 1500, 2000, 2500 µs/cm)

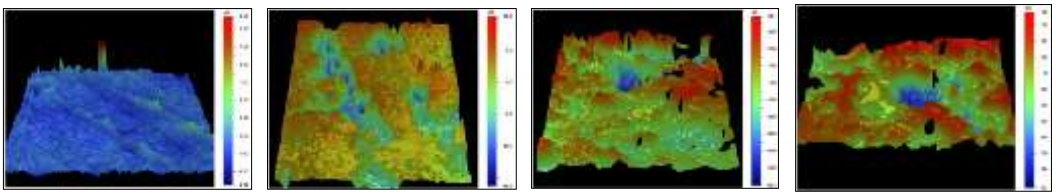

(a). Virgin Sample (b). Aged under AC (c). Aged under +DC (d). Aged under –DC

Figure 3.18. 3-D Images of surface roughness for Sample B with 2500 µS/cm NH4Cl solution

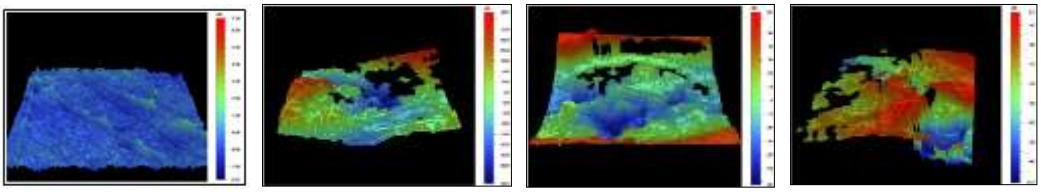

(a). Virgin Sample (b). Aged under AC (c). Aged under +DC (d). Aged under –DC

Figure 3.19. 3-D Images of surface roughness for Sample D with 2500 µS/cm NH4Cl solution

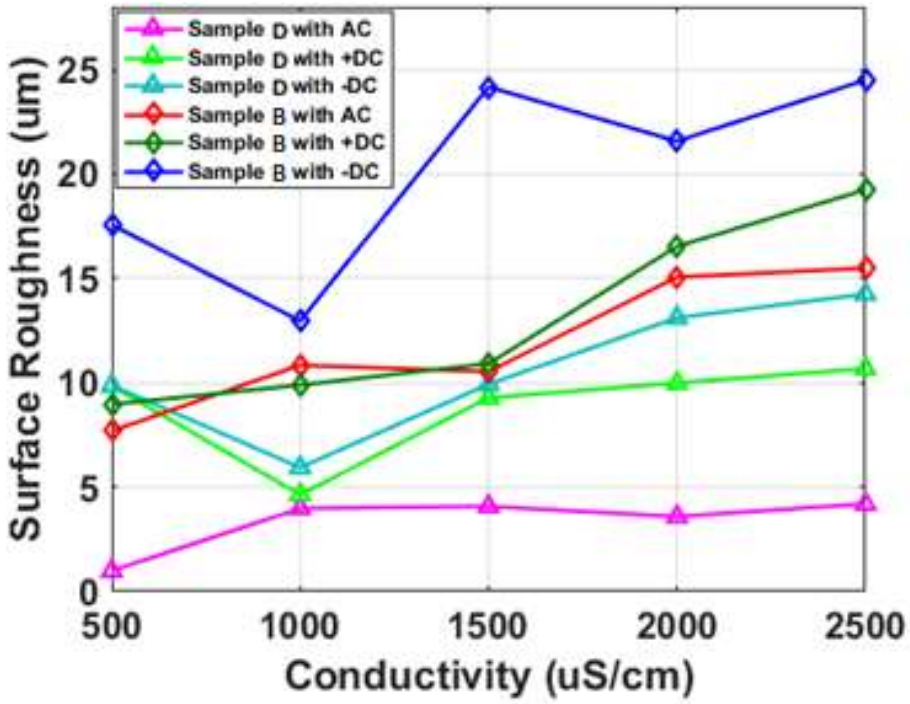

Figure 3.20. Surface Roughness characteristics of Sample B, D for different conductivities

From the figures 3.18, 3.19, surface roughness of insulation is high under negative DC supply than AC and positive DC. By increasing the conductivity of water droplet between the needle electrodes, surface roughness is increasing. Microcomposite material has high surface roughness than nanocomposites for AC, +DC,-DC. Under AC supply degradation of material is less. In 3-D representation blue colour indicates purity and under AC supply it shows green, gold combinations means less degradation but under negative DC, picture full of red means surface degraded heavily. By adding Nano fillers to base epoxy resin, surface degradation decreasing.

3.7. Analysis of discharges using Optical Emission spectroscopy of micro and Nanocomposites

in figures 3.21,3.22 , spectrum was captured by Optical Emission Spectroscopy during arcing with inclined elctrode test by placing 2500 µS/cm conductivity NH_4Cl solution , has shown

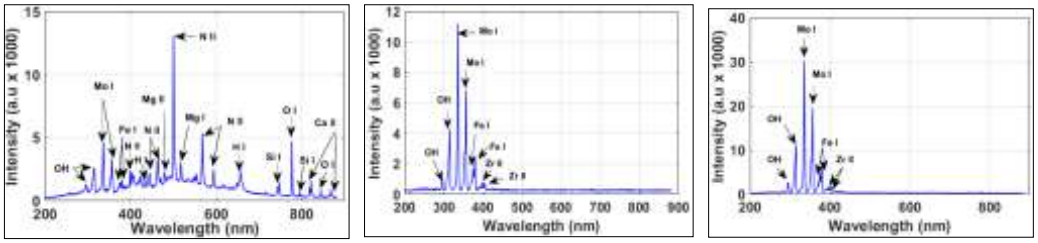

(a). Sample B with AC voltage (b). Sample B with +DC voltage (c). Sample B with -DC voltage

Figure 3.21.. Optical Spectroscopy captured during arcing on Sample B

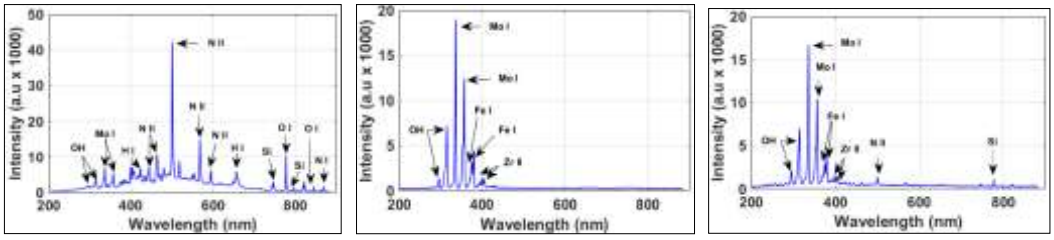

(a). Sample D with AC voltage (b). Sample D with +DC voltage (c). Sample D with -DC voltage

Figure 3.22. Optical Spectroscopy captured during arcing on Sample D

In figure 3.23, it is shown that Local plasma electron temperature obtained based on OES for Sample B and D during continuous arcing under AC, positive and negative DC voltages.

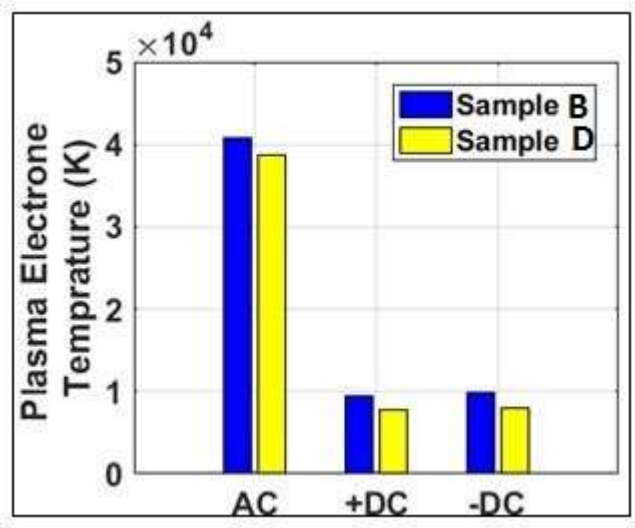

Figure 3.23, Local plasma electron temperature generated while arcing

From the OES studies, Mo , N , Zr , Fe , OH, Si elements has been observed during the arcing process. Under DC supply, The spectral peaks of Sample B and D arcing produce emissions only in the UV wave length region (320 — 470 nm) while peaks recorded under AC supply are spread throughout the entire wavelength range. From the figure 3.23, it is observed that emitted plasma electron temperature under AC supply is higher than positive and negative DC. Temperature levels are nearly same for positive and negative DC. Under all power supplies , emitted plasma electron temperature is high in micro composite than nanocomposite.

3.8. Tensile strength and flexural of epoxy micro and nanocomposites

In figure 3.24, tensile characteristics of epoxy nano and micro composites (tensile stress Vs. Tensile strain) have shown. Both tensile and compressive strength are measured in units of force per unit area- strictly speaking this is “stress”. The SI unit for this is the pascal, Pa, which is N / m^2. The forces involved though are usually so

high that you'll find values typically in kilo pascal (kPa) and mega pascal (MPa). And he strain can be defined as the ratio between the amount of stretching and the original length of the specimen.

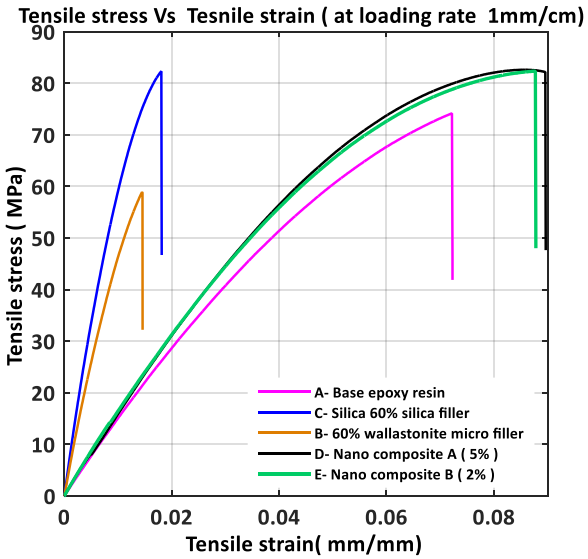

Figure 3.24, Tensile strength characteristic graph of epoxy composites

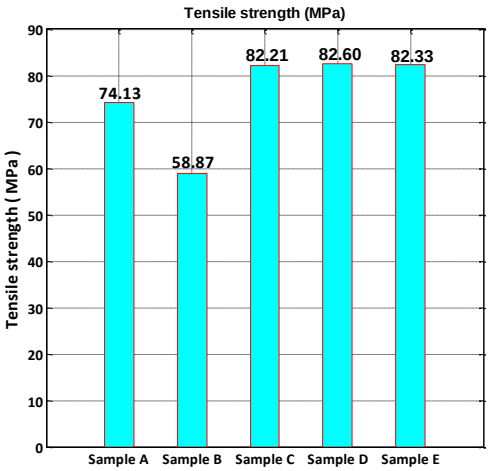

Figure 3.25. Tensile strength of epoxy composites

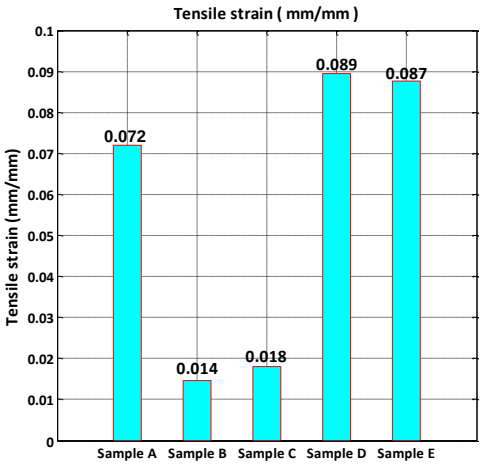

Figure 3.26. Tensile Strain of epoxy composites

From the figure 3.24, it is clearly observed that, 60% wallastonite micro composite material (sample B) has less tensile stress and less tensile strain values than remaining 4 samples. 5% Nano filler composite (sample D) has high tensile stress and high tensile strain values. By adding micro silica filler to base epoxy , its tensile strength increasing but its tensile strain value decreasing. By adding nano fillers with 5% wt , tensile stress and tensile strain values increased means its tensile strength improved . in the other words , in the graph between Tensile stress Vs. Tensile strain, which material has highest area under curve can consider has best mechanical properties.

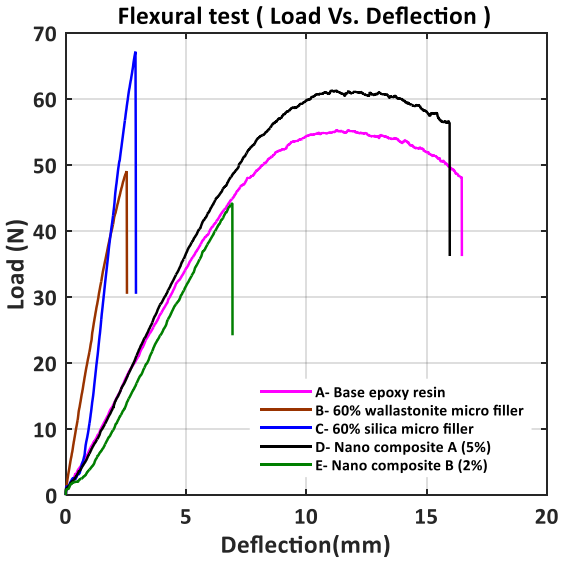

Figure 3.25. Flexural strength characteristics of epoxy composites

From the figure 3.25, it can be concluded that, by adding 60% wallastonite micro fillers to base epoxy resin its load withstand capability decreased and deflection of the material also reduced but by adding 60% fused silica micro filler to base epoxy , its load withstand capability increased by deflection of the

material decreased . so it can be observe that by adding micro fillers , material becoming rigid and stiff so micro composites losing bending capability. 5% nanocomposite material was showing highest load and highest deflection than other materials. 2% nano composite material has lesser loading and bending capacity than base epoxy.

Chapter 4

Conclusion

The important conclusions accrued based on the present study are the following

a. Permittivity and loss factor relies on type of filler. At higher frequencies, the impact of filler content on its permittivity is minimum.

b. Water diffusion test indicate diffusion of water into epoxy nanocomposite is high with nano filler added epoxy resin.

c. Charge accumulation studies indicate that the accumulated charges are high with micro composites. The charge decay occurs fast with nanocomposite material. In addition, it indicates that the filler content have impact on charge accumulation behaviour.

d. Tensile and flexural test clearly indicated the enhanced material properties of the material with nanocomposites compared with micro filler added epoxy resin material.

e. Erosion of material after water droplet test is high with microcompoites compared with nanocomposites. Surface roughness is high in micro composites and less in nano composites after corona discharge studies.

f. The water droplet initiated discharge inception voltage varies with conductivity of the water droplet.

g. The UHF signal radiated during corona discharge process and surface discharge process lies in UHF range with its dominant frequency at 1 GHz.

h. Optical emission spectroscopy is obtained during water droplet initiated discharges. It is realised that the local temperature can rise up to 4000K.

Bibliography

1. Kojima, Y., Usuki, A., Kawasumi, M., Okada, A., Kurauchi, T., Kamigaito, O., 1993b. Sorption of water in nylon 6–clay hybrid. J. Appl. Polym. Sci. 49, 1259–1264

2. T. Tanaka; T. Imai, N. Tagami; M. Okada; N. Hirai; Y. Ohki; ; M. Harada; M. Ochi, Dielectric properties of epoxy/clay nanocomposites - effects of curing agent and clay dispersion method, , IEEE Transactions on Dielectrics and Electrical Insulation, Volume: 15, pp: 24 – 32, 2008

3. T Tanaka (Waseda University), Yoshinobu Mizutani (CRIEPI), Takahiro Imai (Toshiba Corporation), "Digest Report of Investigation Committee on Polymer Nanocomposites and their Applications as Dielectrics and Electrical Insulation" , Electrical Insulating Materials, 2008. (ISEIM 2008). International Symposium.

4. T. Imai ; F. Sawa ; T. Nakano ; T. Ozaki ; T. Shimizu ; M. Kozako ; T. Tanaka, Effects of nano- and micro-filler mixture on electrical insulation properties of epoxy based composites, IEEE Transactions on Dielectrics and Electrical Insulation Vol. 13, No. 1; February 2006

5. T. Imai; Y. Hirano; H. Hirai; S. Kojima; T. Shimizu, Preparation and properties of epoxy-organically modified layered silicate nanocomposites, vol.2, DOI: 10.1109/TDC.2002.11776074

6. T. Imai; F. Sawa; T. Nakano; T. Ozaki; T. Shimizu; M. Kozako; T. Tanaka Effects of nano- and micro-filler mixture on electrical insulation properties of epoxy based composites, IEEE Transactions on Dielectrics and Electrical Insulation Year: 2006, Volume: 13

7. Toshikatsu Tanaka, Zhe Li ,Kenji Okamoto, Yoshimichi Ohki ,"Role of Nano-Filler on Partial Discharge Resistance and Dielectric Breakdown Strength of Micro-Al203 / Epoxy Composites" 2009 IEEE 9th International Conference on the Properties and Applications of Dielectric Materials
8. M. Kozako; N. Fuse; Y. Ohki; T. Okamoto; T. Tanaka, "Surface Degradation of Polyamide Nanocomposites Caused by Partial Discharges Using IEC b Electrodes", IEEE Transactions on Dielectrics and Electrical Insulation Vol. 00, No. 00; Month 2004
9. T. Okamoto T. Tanaka, "Partial discharge pattern recognition for three kinds of model electrodes with a neural network", IEE Proc.-Sri. Meas. Technol., Vol. 142, No. I, January 1995
10. Xingyi Huang; Yong Li; Fei Liu; Pingkai Jiang; Tomonori Iizuka; Kohei Tatsumi; Toshikatsu Tanaka, " Electrical Properties of Epoxy/POSS Composites with Homogeneous", Nanostructure IEEE, Volume: 21, pp: 1516 – 1528, 2014
11. R.Sarathi, R.K.Sahu, T. Tanaka, " understanding the hydrophobic characteristics of epoxy nanocomposites using wavelets and fractal technique"
12. B. Deneve and M.E.R. Shanahan " water absorption by an epoxy resin and its effect on the mechanical properties and infrared spectra " , polymer, vol.34 , pp.5099-5105,1993
13. J. Crank, Mathematics of diffusion OXFORD : clarenson , 2ns edition , 1975
14. Y. DIamant, G. Maron and L.J. Broutman, " the effect of network structure on moisture abosoption of epoxy resin " , J.Appl.poly.sci., Vol.26,.pp.3015-3025,1981
15. Li Shengtao, Yin Guilai, Ni Fengyan, Bai Suna, Li Jianying, Zhang Tuo ,"Investigation on the dielectric properties of nanotitanium dioxide - low density

polyethylene composites", 2010 International Conference on Solid Dielectrics, Potsdam, Germany, July 4-9, 2010

16. Mingze Gao, Peihong Zhang, Feifeng Wang, Lin Li, Zhongyuan Li ,"The Relationship Between Dielectric Properties and Nanoparticle Dispersion of Nano-SILICA/Epoxy Composites" , 2013 Annual Report Conference on Electrical Insulation and Dielectric Phenomena
17. Kremer F., Schonhals A., Luck W. Broadband Dielectric Spectroscopy. Springer-Verlag, 2002
18. Y. Gao, B.X Du and X.H. Zhu "Surface Charging and Charge Decay on Gamma-Ray Irradiated Epoxy Resin Laminate" , 2009 Annual Report Conference on Electrical Insulation and Dielectric Phenomena
19. H. M. Banford, R. A. Fouracre, S. J. MacGregor and M. Judd, "An Investigation of Radiation-Induced Ageing in Cable Insulation Via Loss Measurements at High and Low Frequencies," IEEE Int. Symp. Elect. Insul., pp. 558-561, 1998
20. Y. Gao, B.X. Du, Effect of Gamma-Ray Irradiation on Surface Charge Decay through Bulk of Epoxy Resin"
21. R.Sarathi; V.SriHarsha,water droplet initiated discharges on epoxy nanocomposi tes under DC voltages"
22. T. Kuroyagi, H. Homma, T. Takahashi, K. Izumi, "A fundamental study on the surface degradation of polymer insulation materials in DC voltage application", IEEE Conf. Electr. Insul. Dielectr. Phenomena (CEIDP), pp. 682-685, 1998.
23. R.sarathi, S. aravindh , "Analysis of Surface Discharge Activity in Epoxy Nanocomposites in Liquid Nitrogen under AC Voltage" , IEEE Transactions on Dielectrics and Electrical Insulation Vol. 23, No. 3; June 2016

24. Langland, M., & Cronin, T. (Eds.). (2003). A Summary Report of Sediment Processes in Chesapeake Bay and Watershed. In Water-Resources Investigations Report 03-4123. New Cumberland, PA: U S Geological Survey. Retrieved from http://pa.water.usgs.gov/reports/wrir03-4123.pdf
25. Takahiro imai, Fumio Sawa, Tamon Ozaki, "Effects of epoxy/ filler interface on properties of nano or micro composites"
26. W.F. Hosford, "Overview of Tensile Testing, Tensile Testing", P. Han, Ed., ASM International, 1992, p 1–24
27. P.M. Mumford," Test Methodology and Data Analysis, Tensile Testing", P. Han, Ed., ASM International, 1992, p 49–60
28. Jobin K. Antony, Nilesh J. Vasa',S.R. Chakravarthy, R. Sarathi," Understanding the mechanism of nano-aluminum particle formation by wire explosion process using optical emission technique".
29. R Sarathi, V sriharsha , N.J . Vasa, " water droplet initiated discharges on epoxy nanocomposites under DC voltages " , IEEE transactions on dielectric and electrical insulation, vol.23 , no.13 , june 2016
30. An Xiao ; Simon M. Rowland ; Xin Tu ; J. Christopher Whitehead , "Thermal features of low current discharges and energy transfer to insulation surfaces, IEEE Transactions on Dielectrics and Electrical Insulation (Volume: 21, Issue: 6, December 2014)